Available online at www.sciencedirect.com

ScienceDirect

Procedia CIRP 133 (2025) 644–649

www.elsevier.com/locate/procedia

20th CIRP Conference on Modeling of Machining Operations

Methodology for element selection and clustering in multi-axis directed energy deposition simulation

Severin Maier*,[a], Theo Habenicht[a], Maximilian Hoffmann[a], Haoliang Yu[b], Gernot Mauthner[a], Chong Teng[b], John Fortna[b], Friedrich Bleicher[a]

[a]*Institute of Production Engineering and Photonic Technologies, TU Wien, Getreidemarkt 9, 1060 Vienna, Austria*
[b]*Ansys Inc, 2600 Ansys Dr, Canonsburg PA 15317, United States*

* Corresponding author. Tel.: +43-1-58801-31157. *E-mail address:* severin.maier@tuwien.ac.at

Abstract

Specific modeling techniques are necessary to accurately capture the physical mechanisms for simulating the macroscale thermo-mechanical behavior of an additive directed energy deposition (DED) process. When using the finite element method (FEM) to simulate the DED process, the material deposition typically requires the activation of grouped elements along the deposition path. G-code-based software interfaces usually handle the element grouping (clustering) procedure according to the planned deposition path. However, modern robotic systems often use individualized proprietary controller languages for DED, meaning no generic G-code is available for simulation. A concept that handles the element grouping mechanism without relying on G-code is proposed. The method uses a standardized neutral tool path information from the computer aided manufacturing (CAM) system to automate element grouping. This study demonstrates and analyzes the generally applicable approach for modeling a multi-axis deposition process. The implementation of pre-processing in the FEM as well as the mathematical formulations and methods required for automated element selection and grouping are described.

Keywords: Additive manufacturing (AM); Finite element method (FEM); Computer aided manufacturing (CAM)

1. Introduction

In recent years, Additive Manufacturing (AM) processes have been developed to an advanced level of maturity and have been deployed as a promising technology for many applications in various industries [1, 2]. AM offers numerous advantages in particular for complex near net shaped parts like material and energy efficiency, resulting in significant cost savings. For Metal Additive Manufacturing (MAM) processes, a fundamental distinction can be made between powder bed fusion (PBF) and directed energy deposition (DED) [3, 4, 5]. In the PBF process, the metal powder is deposited layer by layer on the build-up platform and melted by an energy source in the layer-section area of the workpiece geometry according to the used hatch strategy [6, 7]. In DED processes, a feedstock (powder or wire) is melted by a directed energy source (e.g., Wire Laser/Arc Additive Manufacturing – WLAM/WAAM) and deposited onto either the build-up platform or on the previously applied workpiece surface. The material deposition is based on a predefined tool path (deposition track) of the energy source and the material feed unit, which in most cases is represented by the tool center point of a multi-axis robotic system [4, 8].

The overall quality of the above-mentioned MAM processes is significantly affected by a variety of factors including energy input and process parameters such as wire feed speed, dwell times, the volume of powder or wire utilized, hatch strategies, etc. Such interactions between material properties and process parameters involve complex thermo-mechanical behaviors and phase transitions [5]. In order to gain a comprehensive understanding and facilitate the design of MAM processes, it is crucial to utilize and improve process simulation tools, which are currently recognized as the state-of-the-art approach in this field. Process simulation tools can serve as predictive models that enable the investigation of expansive parameter settings and provide key insights into the correlation between the process parameters and the resulting material properties.

10.1016/j.procir.2025.02.110

When using the Finite Element Method (FEM) for simulating the macroscale thermal and mechanical behavior of PBF and DED processes, the modeling has to reflect various process characteristics such as temperature-dependent material properties, realistic boundary conditions (e.g. cooling conditions) or a correct sequence of activating elements following the actual deposition tool path.

One key component when modeling metal additive manufacturing processes is the description of the material build-up process in the simulation. Since the material is deposited over time, the simulation has to consider the thermo-mechanical dependencies. According to the work of Lindgren [9], the deposition modeling technique within FEM systems can be grouped into two categories. Firstly, the “quiet-element-technique” incorporates the entire geometry of the workpiece and all elements in the model. Secondly, the “inactive elements” or “born dead elements” [5, 9] technique continuously adds and includes the deposited geometry and elements into the model. The matrices and element/node connectivity have to be recalculated. In the modeling of subtractive machining processes, similar concepts are often used to deactivate elements and to model material removal [10, 11].

Due to the different process characteristics in the DED process (e.g. higher deposition rate, layer thickness, etc.), the level of model abstraction in macroscale simulation is typically different from PBF to capture the physical mechanisms of the process in an accurate way [5, 8]. Instead of a layer-by-layer technique for PBF processes, elements have to be sequentially activated along the deposition path in DED following a cluster-by-cluster approach [8], see Figure 1a. The build-up geometry is initially meshed and then split into groups of elements (clusters). This procedure of grouping the elements into element clusters according to the deposition tool path is called element clustering. The element clusters can be activated in alignment with respective process parameters such as deposition speed and deposition tool path. Modeling according to such an approach requires an intelligent clustering methodology in order to manage the grouping of elements into clusters and their activation during the process. In addition to the clustering and element activation procedure, a heat source model must also be applied in the DED simulation in order to introduce the local heat load by the arc or laser energy, respectively, to the activated elements. Both, the element clustering methodology as well as the position and orientation of the heat source including the heat load distribution has to be aligned at the predefined deposition tool path. The heat load distribution is usually calculated using a moving coordinate system. For the DED process, Goldak [12] proposed a so-called double ellipsoidal heat source model, which was subsequently modified and extended [5]. Figure 1a shows the application of the modified double ellipsoidal heat source in a DED simulation and in Figure 1b, a simulation of the PBF process can be seen.

To integrate the deposition tool path and process parameter information for MAM modeling in conventional FEM systems, an efficient and standardized methodology is needed to improve industrial acceptance. For standard DED processes, the cluster-by-cluster approach requires that the elements to be added must

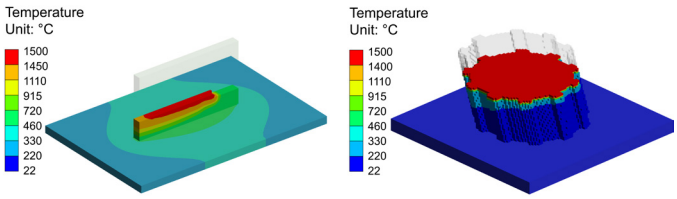

(a) Directed Energy Deposition (DED) (b) Powder Bed Fusion (PBF)

Fig. 1: Thermal FEM-Simulations of different MAM technologies; DED cluster-by-cluster approach (a), PBF layer-by-layer approach (b).

be selected according to the movement of the respective deposition device (tool path). The motion information is transferred in an interpretable format of the machine control, like G-code. For simulation purpose, individually programmed software plug-ins or subroutines enable to integrate the G-code path information in FEM system environments [8, 13, 14, 15].
In most cases of industrial applications in DED processing, robotic systems are used to move the heat source (e.g. welding torch, laser head) in the workspace during the material deposition. Robot manufacturers rely on their individual and proprietary controller language (e.g. KUKA – KRL, ABB – RAPID), rather than on the use of standardized G-code format. While the application of robotic systems is advantageous for industrial applicability of MAM processes, proprietary programming languages limit the utilization of standardized G-code integration, thus impeding a broader application. In order to strengthen the utilization of these process simulation tools, different methodologies involving higher-level tool path planning systems such as computer-aided-manufacturing (CAM) applications are required. These systems utilize 3D model data of the workpiece for virtual process planning. The generated motion- and process information is translated into a specific and machine interpretable format like G-code, robotic-code, etc.

Increased utilization of FEM capabilities in the area of MAM requires more flexibility and efficiency when analyzing varying process strategies. In this paper, a novel approach and methodology for element clustering and coupling between CAM and FEM software systems is presented.

2. Coupling of CAM-FEM

In the proposed approach and methodology, the element clustering as well as the creation of moving coordinate system following the planned tool path is used. A conventional CAM system is directly coupled with the FEM system utilizing the so-called Cutter Location Source file (CLS-file) for the element clustering, as shown in Figure 2.

After the tool path and process parameters have been planned in the CAM software, this information can be converted in a standardized neutral code text file [16]. The standardized Cutter Location (CL) file contains the coordinates of the centerline, the tool for the deposition process will follow [17, 18]. It consists of coordinate system information, tool movement, orientation, and feed commands. Figure 3 depicts

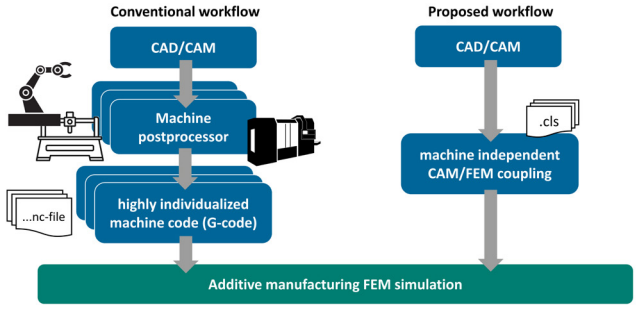

Fig. 2: Proposed approach of CAM-FEM coupling for DED-FEM simulation.

the procedure of the CAM-FEM coupling methodology. The workflow shows the individual steps for a DED process simulation, starting from the CAD/CAM model and ending with a fully defined FEM model of MAM simulation.

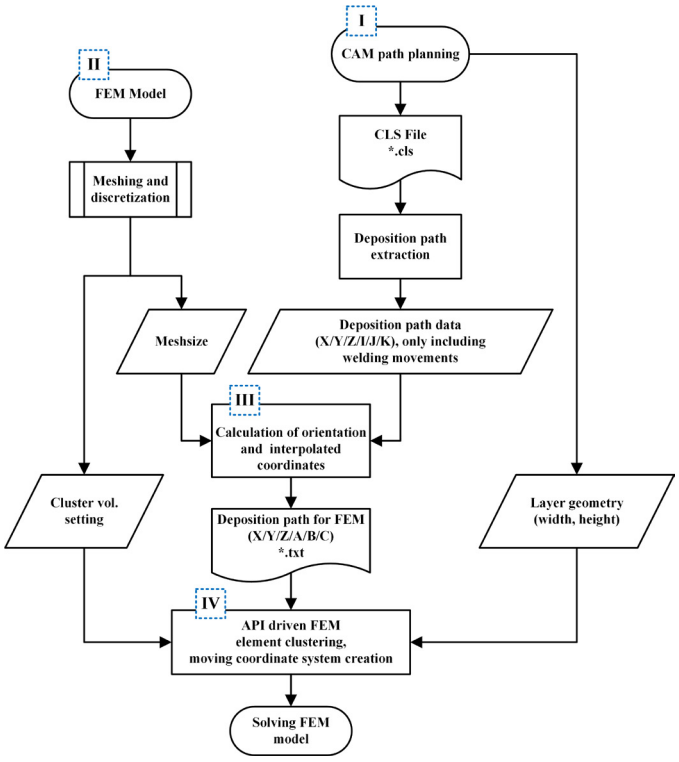

Fig. 3: Workflow diagram of CAM-FEM Coupling.

2.1. CAM and FEM model setup

The workflow of the procedure follows the principle of CAM path planning as the first step (step I in Figure 3). To create the tool path for a given workpiece, the deposition bead cross section (width and height) for the respective process parameters is usually determined with bead models or empirical data [19] to know how many layers and paths are necessary to deposit the material according to the workpiece geometry. With the information of deposition bead geometry and process parameters, the tool path and all robot or machine tool movements can be planned in the CAM environment. The internal CAM commands are then converted to a CLS-file, which can be exported as text format file.

Subsequently, a FEM setup of the CAD workpiece model, which is planned to be build-up, has to be created (step II in Figure 3). For the finite element method, the part needs to be discretized. The element mesh does not need to be a strictly layered mesh with a perfect fit to the workpiece geometry. A Cartesian hexahedral mesh with a feasible fit is recommended, which represents a trade-off between element quality and capturing the workpiece geometry [8]. Such kind of settings can be applied via mesh control settings in the pre-processing step of the FEM software (e.g. Ansys Projection Factor and Mesh Method). In any case, the finite element mesh size, which indicates the length of the finite element edges, have to be properly chosen. When utilizing the proposed CAM-FEM coupling methodology, the smallest element size is necessary as an input for the tool path coordinates manipulation process. A Python script guarantees a full functionality of the algorithm, which is incorporated in step III (Figure 3).

2.2. Extraction and manipulation of deposition path data out of CLS-file

The CLS-file is created by a CAM system and defines the piecewise linear curve through the cutter location (CL) points. Each CL coordinate point is represented by a data format consisting of the path point coordinates. A five-axis command is characterized by a three-dimensional point (X, Y, Z) and the tool axis vector $(I, J, K)^T$. As a first step, the deposition tool path has to be extracted from the CLS-file, where the deposition process occurs. This is done by parsing the CL coordinates according to the PAINT color index command nomenclature, which indicates the motion type [20]. Next, the moving coordinate system has to be created. It consists of the normalized tool feed direction vector $\vec{n}_f$, the tool axis vector $\vec{n}_t = (I, J, K)^T$ and a cross tool feed direction vector $\vec{n}_c$. The tool feed direction vector can be calculated according Equation (1) and indicates the travel direction of the tool along the tool path, whereas the tool axis vector is represented by the $(I, J, K)^T$ vector in the CLS-file. The position vectors $\vec{x}_i$ and $\vec{x}_{i+1}$ represents the three-dimensional path points (X, Y, Z) at previous and subsequent coordinate point, respectively.

$$\vec{n}_f = \frac{\vec{x}_{i+1} - \vec{x}_i}{|\vec{x}_{i+1} - \vec{x}_i|} \tag{1}$$

The vector of the cross-feed $\vec{n}_c$ is thus defined as the cross product $\vec{n}_t \times \vec{n}_f$. In the case of a non-orthogonal relationship between $\vec{n}_f$ and $\vec{n}_t$, the tool axis vector is recalculated using cross product of $\vec{n}_f$ and the calculated $\vec{n}_c$ vector. Consolidating these three vectors, the three orthogonal components of the Cartesian moving coordinate system are fully defined. Depending on the current tool axis and tool feed direction, the orientation of the local moving coordinate system can be described by Tait-Bryan angles with respect to the global stationary coordinate system (cosy). Thus, with the calculations for the intrinsic rotation in Equation 2, the three Tait-Bryan angles A, B and C are also available for every three dimensional coordinate point to

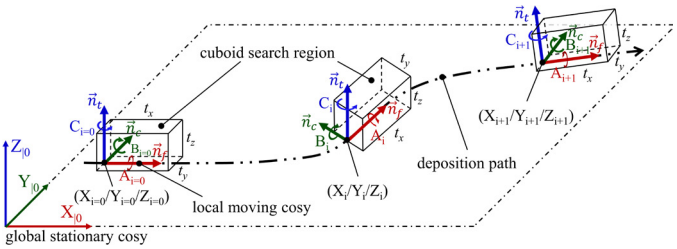

Fig. 4: Cuboid search region moving along deposition path

describe the orientation of the moving coordinate systems, as shown in Figure 4.

$$\begin{aligned} A &= atan2(-n_{t,y}\,,\, n_{t,z}) \\ B &= asin(n_{t,x}) \\ C &= atan2(-n_{c,x}\,,\, n_{f,x}) \end{aligned} \tag{2}$$

Next, the extracted deposition path hast to be manipulated. The selection algorithm follows the path based on the coordinates and searches for elements along the path, adding all those elements that are in the specified range to the current cluster. This means that the coordinates of the deposition path have to be in correlation with the distance of the finite element edge length, so that no elements are skipped during the selection. Additional coordinates $\vec{x}_j$ are inserted in between previous coordinate point $\vec{x}_i$ and the subsequent coordinate point $\vec{x}_{i+1}$ with the given distance dx from the point $\vec{x}_i$ in the direction of the normalized tool feed vector $\vec{n}_f$ (see Equation (3)). Therefore, the meshing process in the FEM software has to be finished before starting the proposed algorithm to know the finite element mesh size, as shown in the workflow (see step II-III in Figure 3).

$$\vec{x}_j = \vec{x}_i + \vec{n}_f \cdot dx \tag{3}$$

After this step, a text file is created including all coordinates of the deposition path with its orientation angles. This file consists of a line structure for each point i indicating the coordinates X/Y/Z/A/B/C, where A, B and C represents the Tait-Bryan angles. In the FEM software, the elements are selected and clustered (see step III-IV in Figure 3).

2.3. Methodology of element selection and clustering

The proposed element selection and clustering into groups can be performed via an Application Programming Interface (e.g. Python API) of the simulation tool.

The proposed element selection method follows the idea of selecting the elements by their element centroid´s position. This requires a defined search region that moves along the deposition path. As depicted in Figure 4, a cuboid search region is used. The algorithm checks the position of each element in order to determine whether it is in the defined cuboid search region or not. Furthermore, the procedure scans the elements and either adds it to the current cluster or skips it. Subsequently, the algorithm checks the next element position. A cluster (named selection or set) is filled with elements of the meshed geometry until the threshold cluster volume is reached and then a new cluster is created. The cluster volume therefore represents the volume of elements, which are activated at once during the simulation per deposition load step and thus represents the deposition process. The cluster volume is a user defined value. It has to be chosen carefully in order to ensure accurate results and keep a reasonable numerical effort for solving.

The position ($X_i/Y_i/Z_i$) of the local coordinate system is read from the text file by the API of the FEM simulation platform. The orientation of the cuboid search region is calculated using the Tait-Bryan angles in order to meet the current orientation of the deposition bead. The dimensions of the cuboid search region represent the dimension of the deposited bead geometry. The width t_y and height t_z of the cuboid should be the same dimension as the bead dimension (layer height, width), which is also used to plan the deposition path in the CAM system.

3. Verification

The approach and methodology were verified using an artificial component. This component consists of a helical deposition bead region, representing the deposited material, encased within an outer cubic body, as illustrated in Figure 5. The concentric double-helical deposition path is indicated as a pink line with a single bead cross section of width t_y = 6 mm and of height t_z = 6 mm, thus a total bead width of 12 mm. The deposition bead profile has a constant roll angle throughout the whole helix, thus representing a multi-axis deposition process. The CAM software Siemens NX was used for tool path planning and the creation of the CLS-file. As described in Figure 3, the deposition path is extracted from the CLS-file and processed using a dedicated Python script. The script calculates the interpolated coordinates and determines the orientation of the moving coordinate system. Mesh generation is carried out using the Ansys FEM simulation platform. Additionally, the element selection and clustering algorithm was implemented in Ansys using the Application Customization Toolkit (ACT), a Python-based API that facilitates workflow automation and the integration of specialized simulation processes.

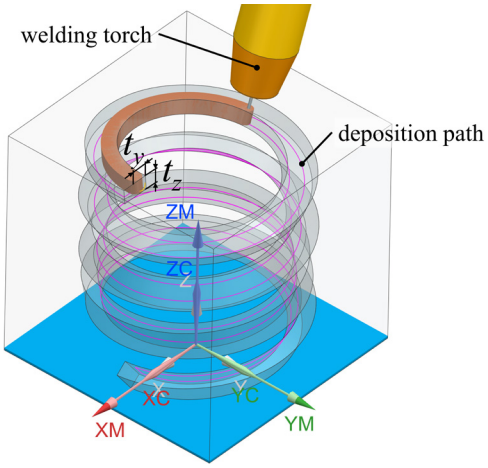

Fig. 5: Artificial helical geometry for multi-axis deposition verification.

The first test was performed to determine how well the volume of the enclosed deposition bead is selected and clustered with different meshing strategies. Four different meshing strategies were used to discretize the cubic body into finite elements. Three Cartesian hexahedral meshes with element sizes of 2, 1 and 0.5 mm (Figure 6a - 6c) and a customized mesh with element size of 2 mm (Figure 6d). Figure 6 shows only the deposition elements for clustering enclosed in the cubic body. The Cartesian mesh was created in alignment with the orientation of the cubic body without any knowledge of the deposition path and consists of regular hexahedral elements. To create the customized mesh, the cubic body geometry was divided into two parts: the helical deposition bead geometry and the remaining cubic body geometry. Then these two parts were meshed with a perfect fit of the elements to their respective geometry.

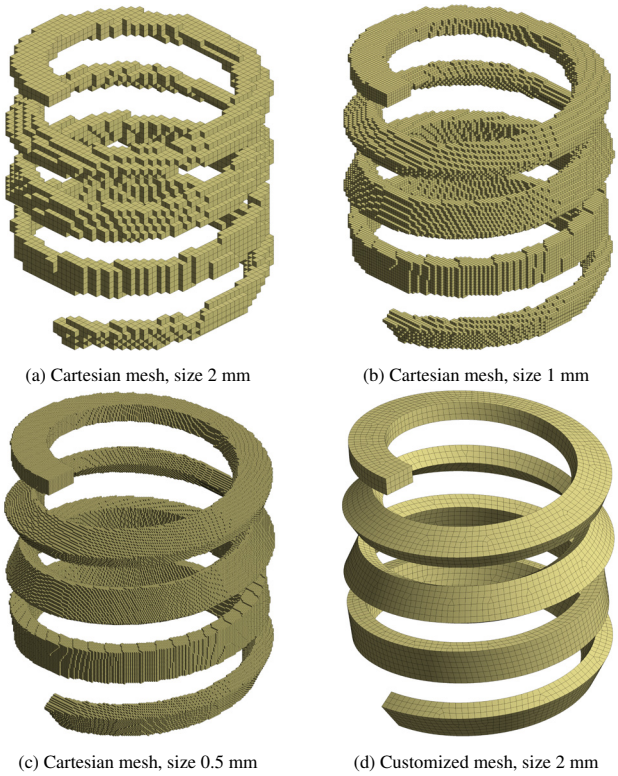

(a) Cartesian mesh, size 2 mm (b) Cartesian mesh, size 1 mm

(c) Cartesian mesh, size 0.5 mm (d) Customized mesh, size 2 mm

Fig. 6: Deposition elements with different mesh strategies and element sizes for verification.

The results of the first test are shown in Figure 7. A clear trend can be seen in the Cartesian meshing. The smaller the element size, the more the discrete volume corresponds to the volume of the helical deposition geometry. However, as the element size decreases, the number of elements in the deposition bead geometry increases at the same time. The accuracy of the Cartesian discretization can be increased at the expense of computing time. As expected, the customized mesh performs best as it fits the geometry exactly.

In the second numerical experiment, the accuracy of the clustering is verified. The clustering algorithm groups the elements along the tool path with the defined search cuboid. After the algorithm has been run, elements remain that could not be clearly assigned to the element groups because they are not located within the search cuboid. In order to be able to compare the different meshes, the ratio of unassigned elements to the total number of elements in the deposition geometry is calculated.

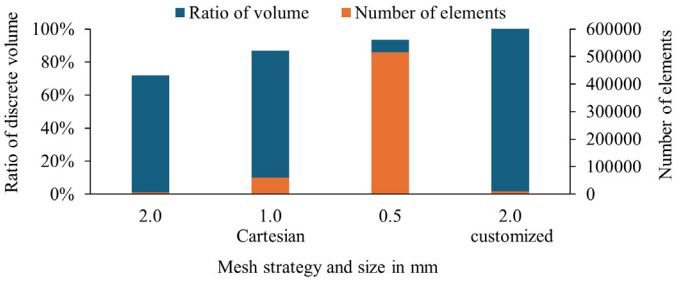

Fig. 7: Ratio of the selected discrete volume and number of elements for each mesh strategy.

Figure 8 shows the comparison between the mesh strategies. Due to the complexity of the component (twisted, unequal edge lengths), it is difficult to create a structured mesh. This is where the general applicable Cartesian mesh shows its strengths. Due to the given structure, the elements are assigned more precisely to the clusters. Also in this verification test, the accuracy increases with decreasing element size.

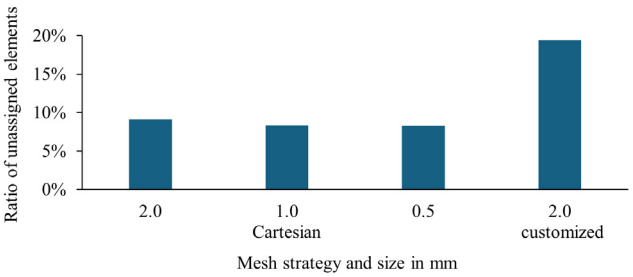

Fig. 8: Ratio of unassigned elements to total number of deposition elements for different mesh strategies.

As described, distances between the path point position vectors $\vec{x}_i$ and $\vec{x}_{i+1}$, respectively are checked in the preparation process (step III in Figure 3) of the raw tool path to guarantee uniform spacing between the path points. This spacing dx between coordinate points can be defined individually for each preparation.

The third experiment will show how the spacing dx affect the clustering algorithm. The meshing strategy “Cartesian 1 mm” was used. In this experiment, the remaining elements that were not clearly assigned by the search cuboid are compared for different spacing values. The results of this test can be seen in Figure 9. The decreasing ratio of unassigned elements with increasing maximum spacing is notable. One explanation for this is that the search cuboid becomes automatically larger with a larger maximum distance, since the length of the cuboid t_x is in correlation with the spacing dx and therefore more elements are assigned directly to the clusters. However, this results also in clusters with larger gaps containing elements which are not connected.

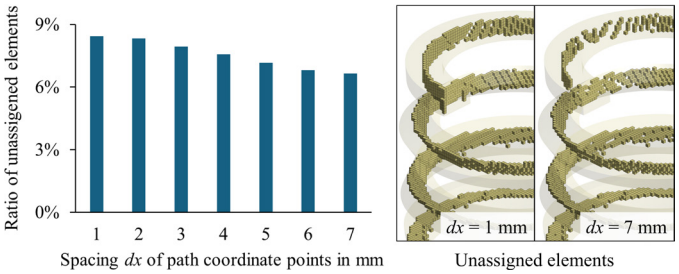

Fig. 9: Ratio of unassigned elements to total number of deposition elements and unassigned elements for different spacing dx.

4. Discussion and outlook

The paper presents an approach and methodology to perform automated element clustering for DED-AM simulation. The novel approach is based on the direct coupling of the CAM system with the FEM software. This could be achieved by using the Cutter Location file. The selection of the elements is based on the centroid position of the respective elements. This ensures a ubiquitously applicable tool, independent of deposition path, mesh strategies and workpiece shape. Furthermore, a simple selection and clustering of the elements is possible even with parallel or concentrical deposition beads, as shown in Figure 5. The numerical complexity must be mentioned as a crucial criterion of the system. The execution time increases with the number of elements of the model, since all elements of the meshed FEM model must be checked according to the demands of the algorithm. An acceleration of the algorithm can be achieved by continuous improvements of the code syntax and advancements in reading and processing the text file, as this has been found to have a major impact on the calculation time. Furthermore a preselection of mesh region might lead to faster clustering.

The two main advantages of the introduced method have been presented by the integration in customized simulation and the independence from the proprietary machine controller language, which means that the methodology can be implemented with any standardized tool path information. The presented clustering approach has been implemented and tested for a multi-axis workpiece geometry in Ansys but the concept can also be used for any other FEM simulation software. Since no G-code is required, it can be used in simulations of DED processes conducted with proprietary robot control languages.

The presented methodology focuses on element activation to simulate the build-up process in AM. Using standard components such as CAM path planning and tool orientation definitions, this approach aligns closely with methods commonly applied in modeling subtractive machining processes. Consequently, the same framework can be adapted to facilitate the selection and deactivation of elements representing material removal during subtractive machining operations. This dual applicability highlights the potential of the approach for automated pre-processing in machining distortion simulations, thereby broadening its utility across both additive and subtractive manufacturing domains.

5. Acknowledgments

This work has been supported and funded by the Austrian Research Promotion Agency (FFG) under project number 888203 in the project Ad-Proc-Add II.

References

[1] B. Barroqueiro, A. Andrade-Campos, R. A. F. Valente, V. Neto, Metal Additive Manufacturing Cycle in Aerospace Industry: A Comprehensive Review, Journal of Manufacturing and Materials Processing 3 (3) (2019) 52.
[2] T.-E. Adams, P. Mayr, The Path from Arc Welding to Additive Manufacturing of Multi-material Parts Using Directed Energy Deposition, BHM Berg- und Hüttenmännische Monatshefte 167 (7) (2022) 318–324.
[3] M.-A. De Pastre, Y. Quinsat, C. Lartigue, Effects of additive manufacturing processes on part defects and properties: a classification review, International Journal on Interactive Design and Manufacturing (IJIDeM) 16 (4) (2022) 1471–1496.
[4] S. Negi, A. A. Nambolan, S. Kapil, P. S. Joshi, M. R., K. Karunakaran, P. Bhargava, Review on electron beam based additive manufacturing, Rapid Prototyping Journal 26 (3) (2019) 485–498.
[5] R. Sampaio, J. Pragana, I. Bragança, C. Silva, C. Nielsen, P. Martins, Modelling of wire-arc additive manufacturing – A review, Advances in Industrial and Manufacturing Engineering 6 (2023) 100121.
[6] D. Dev Singh, T. Mahender, A. Raji Reddy, Powder bed fusion process: A brief review, Materials Today: Proceedings 46 (2021) 350–355.
[7] L. Englert, V. Schulze, S. Dietrich, Concentric Scanning Strategies for Laser Powder Bed Fusion: Porosity Distribution in Practical Geometries, Materials 15 (3) (2022) 1105.
[8] Ansys, Academic Research Mechanical, release 2022 r2 Edition, Help System, Additive Manufacturing, Ansys, Inc., Canonsburg, PA 15317, 2022.
[9] L.-E. Lindgren, H. Runnemalm, M. O. Näsström, Simulation of multipass welding of a thick plate, International Journal for Numerical Methods in Engineering 44 (9) (1999) 1301–1316.
[10] Y. Ma, J. Zhang, D. Yu, P. Feng, C. Xu, Modeling of machining distortion for thin-walled components based on the internal stress field evolution, The International Journal of Advanced Manufacturing Technology 103 (9) (2019) 3597–3612.
[11] J. K. Rai, P. Xirouchakis, Finite element method based machining simulation environment for analyzing part errors induced during milling of thin-walled components, International Journal of Machine Tools and Manufacture 48 (6) (2008) 629–643.
[12] J. Goldak, A. Chakravarti, M. Bibby, A new finite element model for welding heat sources, Metallurgical Transactions B 15 (2) (1984) 299–305.
[13] D. Kovšca, B. Starman, D. Klobčar, M. Halilovič, N. Mole, Towards an automated framework for the finite element computational modelling of directed energy deposition, Finite Elements in Analysis and Design 221 (2023) 103949.
[14] S. Brötz, A. Horr, Framework for progressive adaption of FE mesh to simulate generative manufacturing processes, Manufacturing Letters 24 (2020) 52–55.
[15] B. Edison A, M. Andres, A Directed Energy Deposition Additive Manufacturing Process Simulated with ABAQUS AM Modeler, International Journal of Robotic Engineering 6 (1) (Dec. 2021).
[16] P. Hehenberger, Computerunterstützte Fertigung: Eine kompakte Einführung, Springer Berlin Heidelberg, Berlin, Heidelberg, 2011.
[17] DIN-66215-1:, Programming of numerically controlled machines; CLDATA, general structure and record types (Aug. 1974).
[18] ISO-4343:, Industrial automation systems - Numerical control of machines - NC processor output; Post processor commands (Oct. 2000).
[19] Z. Hu, X. Qin, Y. Li, M. Ni, Welding parameters prediction for arbitrary layer height in robotic wire and arc additive manufacturing, Journal of Mechanical Science and Technology 34 (4) (2020) 1683–1695.
[20] L. T. Tunc, E. Budak, Extraction of 5-axis milling conditions from CAM data for process simulation, The International Journal of Advanced Manufacturing Technology 43 (5-6) (2009) 538–550.